$\beta \Leftrightarrow \beta'$ phase transition with temperature hysteresis in In_2Se_3 films

© S.A. Ponomarev[1,2], N.N. Kurus[1], V.A. Golyashov[1], A.Yu. Mironov[1], D.I. Rogilo[1], A.G. Milekhin[1], D.V. Sheglov[1], A.V. Latyshev[1,2]

[1] Rzhanov Institute of Semiconductor Physics, Siberian Branch, Russian Academy of Sciences, 630090 Novosibirsk, Russia
[2] Novosibirsk State University, 630090 Novosibirsk, Russia

E-mail: ponomarev@isp.nsc.ru

Received April 19, 2024
Revised September 26, 2024
Accepted September 26, 2024

The temperature dependences of Raman scattering for In_2Se_3 films were measured during cooling to the liquid nitrogen temperature and subsequent heating to the room temperature. The Raman spectra show a reversible β-$In_2Se_3 \Leftrightarrow \beta'$-$In_2Se_3$ phase transition with hysteresis in the range of 140–180 K previously discovered by a change in the atomic structure of the surface and the sharp decrease in electrical resistance by a factor of 10^4 during the cooling. The ARPES measurements display changes in film's band structure corresponding to this phase transition.

Keywords: phase transition, In_2Se_3, hysteresis, ARPES, resistance, Raman scattering.

DOI: 10.61011/SC.2024.07.59542.6335H

1. Introduction

After discovery of graphene early in the XXI century and study of its promising properties [1] there gradually emerged and still remains relevant [2,3] an interest in studying the 2-dimensional (2D) materials, in particular, layered metal chalcogenides [4,5]. Layered metal chalcogenides are promising materials for use in microelectronics, photonics and photovoltaics due to the fact that they have semiconductor, metallic, dielectric properties and properties of topological insulators [6]. The near 1 nm thickness of the molecular layers of metal chalcogenides and the presence of a weak Van der Waals bond between them provide high mechanical flexibility and resistance to deformation, creating a potential for use in flexible electronics [7,8]. Due to diversity of physical properties it is possible to use the layered metal chalcogenides for various applications, e.g., MoS_2, Bi_2Te_3 and In_2Se_3 are featuring high electromagnetic emission adsorption coefficient in UV to near infra-red range [9]. As a result, Van der Waals heterostructures based on metal chalcogenides have a huge potential for using their electronic and optoelectronic properties in the design of functional devices such as tunnel transistors, recording and storage devices, photodetectors, solar cells, and etc. [10]. One of the most prominent representatives of the metal chalcogenides is layered In_2Se_3, which is promising for creation of solar photo-cells, photodetectors and memory devices on its base [6,11,12].

A number of metal chalcogenides, and in particular In_2Se_3, are characterized by the presence of polymorphic modifications (phases) having the same stoichiometry, but having different structural and electronic properties. For instance, recently at least eight phases In_2Se_3 have been experimentally found and theoretically predicted, and not all of them are layered [11–13]. However, taking into account the stability of phases in normal conditions and their well-known electrical and physical properties, α-, β- and γ-In_2Se_3 phases are worth mentioning in terms of their practical use; other In_2Se_3 phases are unstable in normal conditions [12,14–16].

In_2Se_3 is known to have several phase transitions changing its properties, e.g., with the temperature rise within 323–473 K, corresponding to phase transition α-$In_2Se_3 \Rightarrow \beta$-$In_2Se_3$, a resistance jump by 3 orders of magnitude can be observed [15]. This phase transition makes its possible to use In_2Se_3 as a basis for creation of data storage devices [17]. Recently, the method of scanning tunneling microscopy within the temperature range of 140–180 K has been used that allowed registering for the first time the phase transition $\beta \Leftrightarrow \beta'$-$In_2Se_3$ [14], where, based on the *ab initio* analysis, one layer of β'-In_2Se_3 was predicted to have a band gap by 0.45 eV wider than one layer of β-In_2Se_3; at that, it was noted that the increase in the number of layers results in the band gap narrowing from 2.06 to 1.42 eV for β'-In_2Se_3 and from 1.62 to 1.15 eV for β-In_2Se_3. However, in the later study [18] with the use of the angle-resolved photo-emission spectroscopy (ARPES) the measured width of the band gap of the bulk β'-In_2Se_3 was ~ 0.97 eV, while in the study [19] with the use of APRES method it was demonstrated, visa versa, that the band gap becomes wider with the increase of the number of β-In_2Se_3 layers. Paper [20] outlines the measurement of temperature dependence of β-In_2Se_3/Si(111) film resistance, which demonstrates the resistance hysteresis within the range of 140–180 K. When the sample of room temperature was cooled down to about 140 K a drastic decline of resistance by a factor of $\sim 10^4$ was observed, and reverse transition occurred

with further heating of the sample > 180 K. Thus, this phase transition was registered by different methods and different author groups, but the published data have a number of contradictions. Due to the studied properties of β- and β'-In_2Se_3 phases and transition between them a number of models of the atomic structure of phase β'-In_2Se_3 were published [12,14,18,19,21]. However, a reasonable choice of the correct model requires a comprehensive analysis of the data obtained by the largest number of different experimental methods, as well as their modeling by appropriate analysis methods *ab initio*.

This paper outlines the Raman scattering spectra experimentally measured during cooling of β-In_2Se_3/Si(111) film to the temperature of liquid nitrogen and its heating to the room temperature with a 10 K, increment, demonstrating the phase transition $\beta \Leftrightarrow \beta'$-$In_2Se_3$. Angular resolution photo-emission spectra with at room temperature and liquid nitrogen temperature were measured for the first time.

2. Experimental and measuring technique

In_2Se_3 film was grown on Si(111) substrate of *n*-type ($0.3\,\text{Ohm}\cdot\text{cm}$) with a size of $7 \times 1 \times 0.38$ mm in the column *in situ* of the reflection electronic microscope (REM) using an evaporator, providing the possibility of both, individual and joint thermal evaporation of selenium and indium, forming the molecular beams of selenium and indium [22]. The sample was heated by passing electric current through it. Si(111) surface was cleaned by annealing at a temperature of 1300°C for 10 minutes. Selenium flow was calibrated by the rate of disappearance of Si(111)-7×7 RHEED patterns at a temperature of 450°C during formation of the selenium-induced surface phase „1×1“ [23,24] with selenium covering of 1/2 ML ($1\,\text{ML} = 7.8 \cdot 10^{14}\,\text{cm}^{-2}$). Indium flow was calibrated by the rate of formation of $\sqrt{3} \times \sqrt{3}$ reconstruction on Si(111)-7×7 surface at 450°C, formed during indium covering of 1/3 ML [25]. In experiment the In/Se flows ratio in the range of $1/6-1/3$ was used, when In_2Se_3 film is growing with the lowest defects concentration [26]. After calibration of In and Se flows the superstructure Si(111)-7×7 was removed by absorption of 1/3 ML of indium onto Si(111) surface at 450°C in order to form $\sqrt{3} \times \sqrt{3}$ superstructure followed by the sample heating up to the temperature of 600°C at which indium is sublimated leaving an atomic-pure non-reconstructed surface Si(111)-1×1 [27]. However, on such Si(111) surface the broken covalent bonds are present, preventing the formation of layered In_2Se_3 with a Van der Waals bond with the substrate which results in the necessity of passivation of Si(111) surface prior to initiating the growth of In_2Se_3. Paper [28], describes the process of passivation of the surface by chalcogen (Te) atoms closing the covalent bonds with formation of dimers. At the same time, selenium, like tellurium, is a chalcogen, and in this experiment it is the most acceptable for passivation of broken bonds: adsorption of 1 ML selenium was carried out at a temperature of 100°C. In paper [27] it was demonstrated that, by initiating the growth of layered $SnSe_2$ through crystallization of the amorphous layer it is possible to achieve low concentration of defects in the film. Similar process was implemented in this study, as well: after the surface had been passivated with selenium atoms a 1 nm thick amorphous In_2Se_3 layer was deposited, after which through rapid heating to the growth temperature (450°C) this amorphous layer was crystallized and further epitaxial growth of In_2Se_3 with a minimum thickness of 10 nm took place (because of RS spectrometer sensitivity limit). The growth was controlled by observing the reflected high-energy electron diffraction (RHEED) patterns. With the appearance of point reflections peculiar to the 3D island growth, the flow of indium ceased and the sample was cooled down to the room temperature in the presence of molecular flow of selenium, after which ~ 10 nm of selenium was deposited to prevent the reaction of In_2Se_3 film with the atmosphere during its further moving to ARPES system for study of the band structure. After that, the obtained film was studied by methods of Raman scattering (RS) and *ex situ* atomic-force microscopy (AFM).

The electronic structure of the obtained film surface was measured by ARPES method using the ultrahigh-vacuum system of photoelectron spectroscopy SPECS ProvenX-ARPES, fitted with a hemispherical electrons energy analyzer ASTRAIOS-190 with electrostatic deflector and non-monochromatic helium gas-discharge lamp UVS-300 (emission HeIα, $h\nu = 21.22$ eV). The structure and chemical composition of the sample surface were controlled by low-energy electron diffraction (LEED) and X-ray photoelectron spectroscopy (XPS) methods, respectively. Raman scattering spectra were measured by Horiba Xplora plus spectrometer at excitation with a 532 nm wavelength laser. An atomic force microscope Bruker Multimode 8 was used to study the surface morphology of the structure.

3. Experimental results

In column *in situ* of the reflection electronic microscope In_2Se_3 film with a nominal thickness of ~ 20 nm was grown on Si(111) surface. After that, using the AFM method the image of the film surface morphology was obtained (Figure 1), where we may see the islands of layered In_2Se_3 with lateral sizes of $1-3\,\mu$m and height of 10–15 nm, which is consistent with the reflected high-energy electron diffraction (RHEED) patterns as smooth elongated streaks observed during the experiment (see insert window in Figure 1). In the scaled-up image of the layered island surface (Figure 1, in the right) we may see the atomic flat terraces separated by atomic steps ~ 1 nm high which is consistent with the known data about molecular layer In_2Se_3 [13]. The islands have low concentration of dislocations with a screw component ($\sim 2\,\mu\text{m}^{-2}$).

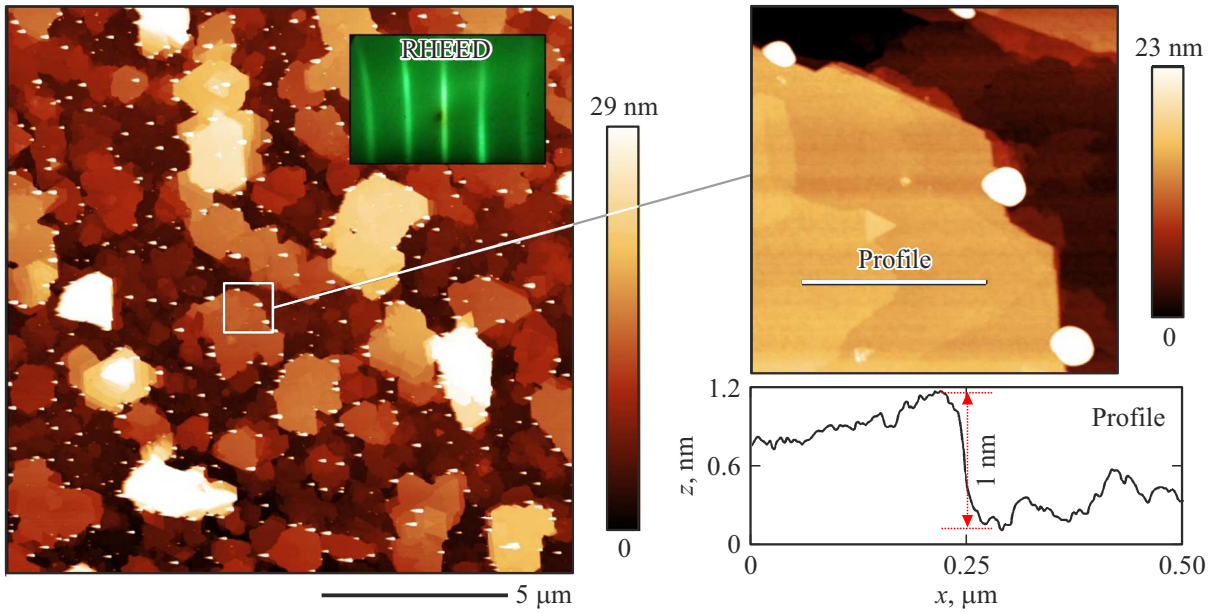

Figure 1. AFM-image of In_2Se_3 film surface. Insert window in the figure — RHEED pattern during growth). From the right: scaled-up fragment of an image of 3D island with a profile obtained across the atomic step In_2Se_3 with a height of 1 nm. (A color version of the figure is provided in the online version of the paper).

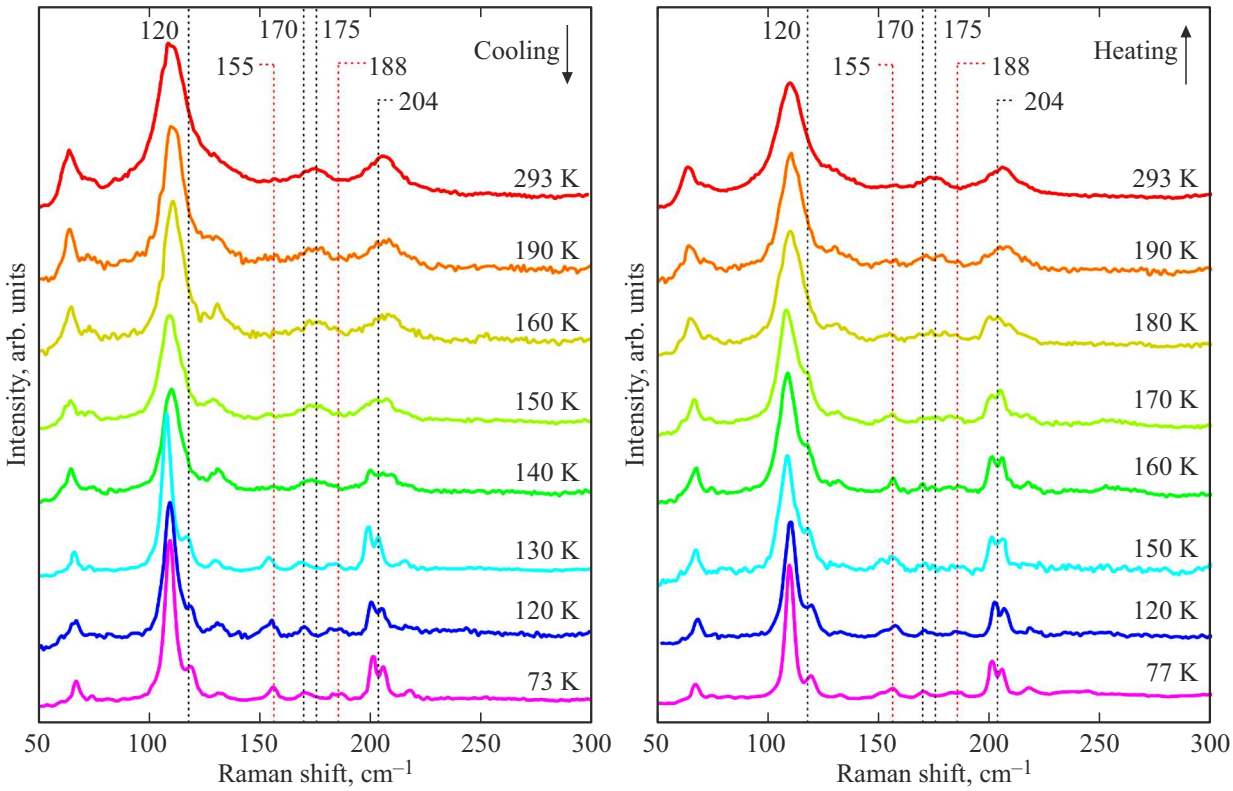

Figure 2. Raman scattering spectra of In_2Se_3 film in the area of $\beta' \Leftrightarrow \beta$-$In_2Se_3$ phase transition during cooling and heating.

RS spectra were measured during the sample cooling to 77 K and further heating up to the room temperature (Figure 2). When cooling down to ~ 140 K at frequency 175 cm^{-1} the peak corresponding to the oscillation mode β-In_2Se_3 [29], disappeared and the three peaks were simultaneously observed at frequencies of 155, 170 and 188 cm^{-1} for the first time. Also, in the curves a branch at 120 cm^{-1} and a distinct doublet structure at 204 cm^{-1} are observed.

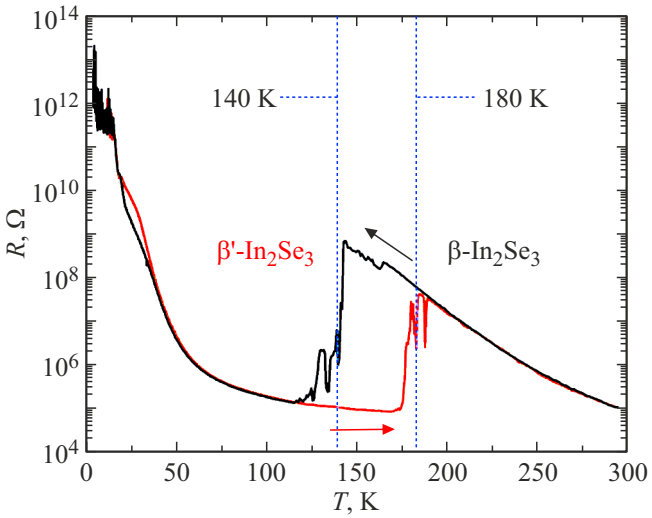

Figure 3. Hysteresis of resistance of In_2Se_3 film in the area of $\beta \Leftrightarrow \beta$-$In_2Se_3$ phase transition during cooling and heating.

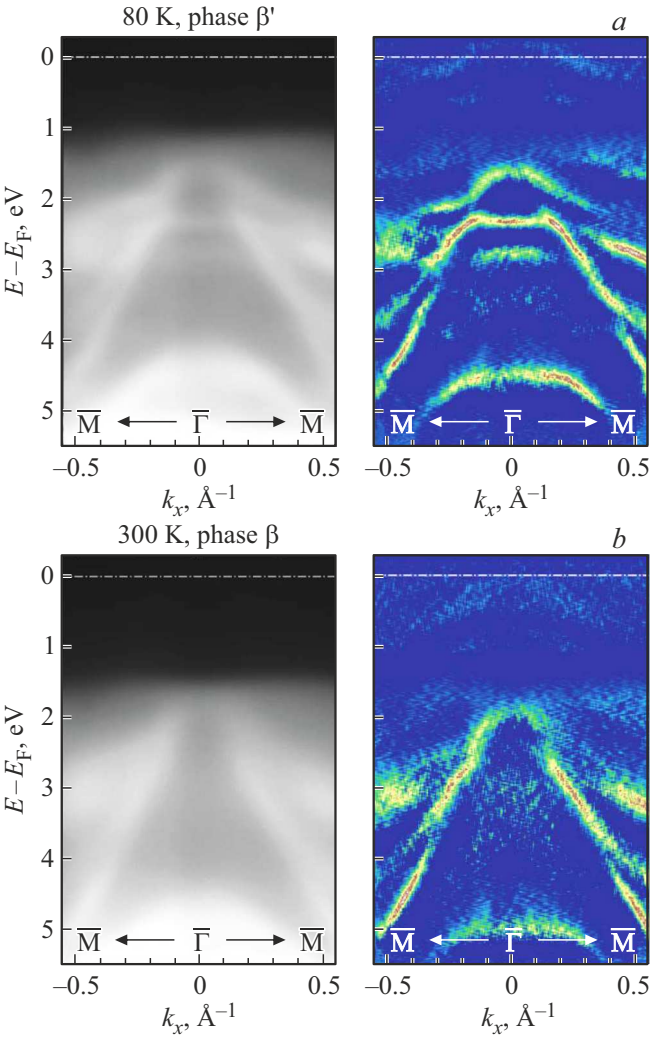

Figure 4. The electronic states dispersion patterns on the surface of In_2Se_3, film were obtained by ARPES method in M–G–M section at the sample temperature of 80 K (*a*) and 300 K (*b*). From the left — photo-emission spectra, in the right — corresponding „curvature“ spectra patterns.

With the following film heating to a temperature above ~ 180 K the initial spectra started to recover: the distinct branch and the doublet structure at 120 and 204 cm^{-1} disappeared along with disappearance of three peaks at 155, 170 and 188 cm^{-1} and the following occurrence of the peak at 175 cm^{-1}. Thus, the observed phase transition is a reversible one and in terms of hysteresis temperature it corresponds to transition β-$In_2Se_3 \Leftrightarrow \beta'$-$In_2Se_3$ (Figure 3), registered in papers [14,20].

The observed phase transitions should also be manifested as dispersion of the electronic states of the studied films. Figure 4, *a* shows a valence band dispersion pattern near point G (G) of Brillouin zone of the surface of In_2Se_3 sample obtained by ARPES method after annealing of initial structure $Se/In_2Se_3/Si(111)$ in vacuum at ~ 650 K for 15 min and its fast (< 3 min) cooling to a temperature of 80 K which resulted in formation of β'-In_2Se_3 phase. Photo-emission from the electronic states of the conduction band within the entire Brillouin zone was not observed in the spectra. At that, the valence band top lies beneath Fermi level by 0.9 eV, which corresponds to the width of indirect band gap of the bulk β'-In_2Se_3 [18], and indicates *n*-type of the obtained film conductivity, and, thus, may explain a drastic reduction of the film resistance by a factor of 10^4 during phase transition $\beta \Rightarrow \beta'$ (Figure 3). To highlight the features of the dispersion of valence band states, Figure 4, *a* on the right shows „curvature“ pattern of the photoelectronic spectrum obtained using the procedure presented in [30].

Upon subsequent heating of the sample to 300 K, the dispersion of valence band states undergoes significant changes (Figure 4, *b*). The valence band top is shifted towards higher bond energies and is located by ~ 1.5 eV lower than Fermi level, which corresponds to a wider band gap during transition β'-$In_2Se_3 \Rightarrow \beta$-$In_2Se_3$ [19,31]. However, it should be noted that these changes may also be associated with a change in the surface potential and a corresponding change in bands surface curvature due to heating of the sample. We may see, that with the temperature rise the bands dispersion greatly varies within the range of 2–3 eV bond energies. In particular, during transition β'-$In_2Se_3 \Rightarrow \beta$-$In_2Se_3$ the additional branches of electron- and hole-type states vanish. The observed changes may indicate the changes in symmetry of a unit cell In_2Se_3. Despite the fact that currently we have several models of atomic structure of β'-In_2Se_3 phase [12,14,18,19,21], no calculations of the band structure and oscillations spectrum for this low-temperature phase have been carried out, therefore, we cannot distinguish the most precise model among them.

4. Conclusion

Raman scattering spectra for In_2Se_3 film were first measured when cooling down to 77 K and further heating up to the room temperature. A hysteresis corresponding

to the reversible phase transition β-$In_2Se_3 \Leftrightarrow \beta'$-$In_2Se_3$ was discovered. When cooling down to a temperature of ~ 140 K we could see vanishing of the peak at 175 cm^{-1}, corresponding toβ-In_2Se_3, with simultaneous occurrence of peaks at 155, 170 and 188 cm^{-1}, a distinct branch at 120 cm^{-1} and a clearly visible doublet of structure at 204 cm^{-1}. When heating > 180 K the RS spectrum is restored to the initial one. According to ARPES, in transition β'-$In_2Se_3 \Rightarrow \beta$-$In_2Se_3$ the valence band top is shifted from 0.9 eV towards higher bond energies and is located ~ 1.5 eV lower than Fermi level, which corresponds to the increased width of β-In_2Se_3 band gap during phase transition β'-$In_2Se_3 \Rightarrow \beta$-$In_2Se_3$. At that, β' phase has a *n*-type conductivity, which may explain a drastic decrease of the film resistance during transition $\beta \Rightarrow \beta'$. The obtained experimental data supplement the available information about phase transition $\beta \Leftrightarrow \beta'$: hysteresis of resistance of In_2Se_3 film with a decline by a factor of $\sim 10^4$ and atomic structure of In_2Se_3 surface.

Funding

This paper was supported financially by the Russian Science Foundation (grant No. 22-72-10124) with the use of „Nanostructures“ equipment provided by the Shared Research Facility.

Conflict of interest

The authors declare that they have no conflict of interest.

References

[1] A.K. Geim, K.S. Novoselov. Nature Materials, **6** (3), 183 (2007).
[2] K.S. Novoselov, D. Jiang, F. Schedin, T.J. Booth, V.V. Khotkevich, S.V. Morozov, A.K. Geim. Proc. Natl. Acad. Sci., **102** (30), 10451 (2005).
[3] A.K. Geim, I.V. Grigorieva. Nature, **499** (7459), 419 (2013).
[4] K. Zhang, T. Zhang, J. You, X. Zheng, M. Zhao, L. Zhang, J. Kong, Z. Luo, S. Huang. Small, **20** (19), 2307587 (2024).
[5] A. Giri, G. Park, U. Jeong. Chem. Rev., **123** (7), 3329 (2023).
[6] S. Vishwanath, X. Liu, S. Rouvimov, L. Basile, N. Lu, A. Azcatl, K. Magno, R. Wallace, M. Kim, J. Idrobo, J. Furdyna, D. Jena, H. Xing. J. Mater. Res., **31** (7), 900 (2016).
[7] Z. Yang, J. Hao. Adv. Mater. Technol., **4** (8), 1900108 (2019).
[8] W. Zheng, T. Xie, Y. Zhou, Y. Chen, W. Jiang, S. Zhao, J. Wu, Y. Jing, Y. Wu, G. Chen, Y. Guo, J. Yin, S. Huang, H. Xu, Z. Liu, H. Peng. Nature Commun., **6**, 6972 (2015).
[9] F. Xia, H. Wang, D. Xiao, M. Dubey, A. Ramasubramaniam. Nature Photonics, **8** (12), 899 (2014).
[10] W. Liao, Y. Huang, H. Wang, H. Zhang. Appl. Mater. Today, **16**, 435 (2019).
[11] W. Li, F.P. Sabino, F. Crasto de Lima, T. Wang, R.H. Miwa, A. Janotti. Phys. Rev. B, **98** (16), 165134 (2018).
[12] J. Li, H. Li, X. Niu, Z. Wang. ACS Nano, **15** (12), 18683 (2021).
[13] X. Tao, Y. Gu. Nano Lett., **13** (8), 3501 (2013).
[14] F. Zhang, Z. Wang, J. Dong, A. Nie, J. Xiang, W. Zhu, Z. Liu, C. Tao. ACS Nano, **13** (7), 8004 (2019).
[15] C. Julien, M. Eddrief, M. Balkanski, E. Hatzikraniotis, K. Kambas. Phys. Status Solidi, **88** (2), 687 (1985).
[16] H. Li, J. Luo, J. Zhang, X. Shi. J. Phys. Chem. C, **127** (46), 22510 (2023).
[17] J. Igo, M. Gabel, Z. Yu, L. Yang, Y. Gu. ACS Appl. Nano Mater., **2** (10), 6774 (2019).
[18] J.L. Collins, C. Wang, A. Tadich, Y. Yin, C. Zheng, J. Hellerstedt, A. Grubisic-Cabo, X. Tang, S. Mo, J. Riley, E. Huwald, N. Medhekar, M. Fuhrer, M. Edmonds. ACS Appl. Electron. Mater., **2** (1), 213 (2020).
[19] Q. Meng, F. Yu, G. Liu, J. Zong, Q. Tian, K. Wang, X. Qiu, C. Wang, X. Xi, Y. Zhang. Nanomaterials, **13** (9), 1533 (2023).
[20] S. Ponomarev, D. Rogilo, A. Mironov, D. Sheglov, A. Latyshev. 2021 IEEE 22nd Int. Conf. of Young Professionals in Electron Devices and Materials (EDM), **2021** (18), 50 (2021).
[21] J. Liang, H. Jin, J. Zhang, X. Chen. J. Phys.: Conf. Ser., **1622** (1), 4 (2020).
[22] A.V. Latyshev, L.I. Fedina, D.I. Rogilo, S.V. Sitnikov, S.S. Kosolobov. *Atomically Controlled Silicon Surface* (Parallel, Novosibirsk, 2016). ISBN978-5-98901-188-9,-0
[23] D.I. Rogilo, L.I. Fedina, S.A. Ponomarev, D.V. Sheglov, A.V. Latyshev. J. Cryst. Growth, **529**, 125273 (2020).
[24] S.A. Ponomarev, D.I. Rogilo, A.S. Petrov, D.V. Sheglov, A.V. Latyshev. Optoelectron. Instrum. Data Process., **56** (5), 449 (2020).
[25] A.V. Zotov, A.A. Saranin, O. Kubo, T. Harada, M. Katayama, K. Oura. Appl. Surf. Sci., **159–160**, 237 (2000).
[26] B. Thomas. Appl. Phys. A: Solids Surf., **54** (3), 293 (1992).
[27] S.A. Ponomarev, K.E. Zakhozhev, D.I. Rogilo, A.K. Gutakovsky, N.N. Kurus, K.A. Kokh, D.V. Sheglov, A.G. Milekhin, A.V. Latyshev. J. Cryst. Growth, **631**, 127615 (2024).
[28] D. Dragoni. Phys. Rev. B, **106** (19), 1 (2022).
[29] L. Liu, J. Dong, J. Huang, L. Liu, J. Dong, J. Huang, A. Nie, K. Zhai, J. Xiang, B. Wang, F. Wen, C. Mu, Z. Zhao, Y. Gong, Y. Tian, Z. Liu. Chem. Mater., **31** (24), 10143 (2019).
[30] P. Zhang, P. Richard, T. Qian, Y.-M. Xu, X. Dai, H. Ding. Rev. Sci. Instrum., **82** (4), 043712 (2011).
[31] Z. Lu, G.P. Neupane, G. Jia, H. Zhao, D. Qi, Y. Du, Y. Lu, Z. Yin. Adv. Funct. Mater., **30** (40), 1 (2020).

Translated by T.Zorina